Optical Materials 84 (2018) 536–544

Contents lists available at ScienceDirect

Optical Materials

journal homepage: www.elsevier.com/locate/optmat

Solvothermal synthesis and luminescent properties of hierarchical flowerlike $ZnAl_2O_4$:Ho^{3+} microstructures

F. Femila Komahal[a,b], H. Nagabhushana[c,*], R.B. Basavaraj[c], G.P. Darshan[d], B. Daruka Prasad[e]

[a] Department of Physics, Government Science College, NT Road, Bangalore, 560 001, India
[b] Research and Development Center, Bharathiar University, Coimbatore, 641 046, India
[c] Prof. C.N.R. Rao Centre for Advanced Materials Research, Tumkur University, Tumkur, 572 103, India
[d] Department of Physics, Acharya Institute of Graduate Studies, Bangalore, 560 107, India
[e] Department of Physics, BMS Institute of Technology and Management, VTU-affiliated, Bangalore, 560 064, India

ARTICLE INFO

Keywords:
Photoluminescence
Thermoluminescence
Bio-surfactant
Dosimetry applications

ABSTRACT

Hierarchical microstructures of $ZnAl_2O_4$:Ho^{3+} (0.25–5 mol %) nanophosphors (NPs) were synthesized via solvothermal route using *Epigallocatechin gallate* (EGCG) as a bio-surfactant. The effect of EGCG concentration on the morphology was studied in detail. The Powder X-ray diffraction (PXRD) studies confirm the cubic phase of the samples. The photoluminescence (PL) emission spectra exhibit peaks at ~ 540, 553 and 666 nm were due to transitions $^5F_4 \rightarrow {}^5I_8$, $^5S_2 \rightarrow {}^5I_8$ and $^5F_5 \rightarrow {}^5I_8$ of Ho^{3+} ions, respectively. Thermoluminescence (TL) properties of $ZnAl_2O_4$: Ho^{3+} (0.25–5 mol %) NPs were studied after exposure of ^{60}Co γ-rays at a warming rate of 6 °Cs^{-1}. The TL intensity was found to increase with γ-dose. The kinetic parameters have been determined using Chen's method from the deconvoluted glow curve. The CIE Chromaticity co-ordinates of all the prepared phosphors were located in the blue region. The above results clearly evident that the optimized Ho^{3+} activated $ZnAl_2O_4$ NPs was a promising single phased phosphor for WLED's and dosimetry applications.

1. Introduction

In the recent years, increased worldwide interest in both green synthesis and nanotechnologies [1], more sustainable manufacturing routes to crystalline nanometric inorganic materials. The vast majority of published literature on the syntheses of nanoparticles (NPs) relates to materials prepared under static or batch processes [2] or using multi-step processes. More recently, there is an increasing number of publications which demonstrated the potential of rapid and continuous methods for controlled manufacture of inorganic nanomaterials [3–5].

The rare earth doped NPs have been paid much attention owing to their high thermal stability, superior catalytic, electrical and optical properties [6]. In contradiction to the analogous bulk samples, nanoscopic phosphors present the following advantages: (i) high packing density, (ii) low light-scattering effects, (iii) shorter preparation time, (iv) lower sintering temperatures (when necessary), and (v) they are easily suspendable in liquid media. Reducing crystal size, physical phenomena which are not noticeable in macro/microdimensions, e.g., quantum mechanical effects, can be highlighted, influencing the optical properties of nanostructured semiconductors [7].

Over the past few decades, many researchers have been focused on the fabrication of efficient luminescent nanophosphors due to its wide range of applications on display, solar cells, catalysts, sensors, etc. [8]. Among them, nano zinc aluminate ($ZnAl_2O_4$) has been found to be an efficient host material with a wide optical band gap (~3.8 eV), high thermal and chemical stability, high mechanical resistance, low acidity, hydrophobicity and the possibility of generating broadband emission. Due to its transparency and electro conductive properties, it can be used for ultraviolet (UV) photo electronic devices [9]. Commonly, the $ZnAl_2O_4$ was fabricated by various routes, namely, solid-state reaction, co-precipitation, hydrothermal, microwave, solvothermal, combustion, and sol– gel methods. Among these routes, the green approach and most promising can be considered is the solvothermal synthesis processes due to its improvement of producing pure and ultrafine powders [10].

In the present work, a simple solvothermal method has been followed for the preparation of the Ho^{3+} ions doped $ZnAl_2O_3$ using EGCG as a bio-surfactant. The obtained samples were well characterized by means of PXRD, SEM, TEM, DRS, PL and TL. The effect of *EGCG* surfactant concentration on morphology of the sample was studied in detail. The kinetic parameters, namely activation energy (E), order of kinetics (b) and frequency factor (s) were estimated by TL glow curves

* Corresponding author.
E-mail addresses: bhushanvlc@gmail.com (H. Nagabhushana), darukap@bmsit.in (B. Daruka Prasad).

https://doi.org/10.1016/j.optmat.2018.06.058
Received 1 February 2018; Received in revised form 23 June 2018; Accepted 25 June 2018

using Chen's peak shape method and glow curve deconvolution (GCD) functions.

2. Experimental

2.1. Solvothermal synthesis of $ZnAl_2O_4$: Ho^{3+} (0.25–5 mol %) NPs

The $ZnAl_2O_3$:Ho^{3+} (0.5–5 mol %) NPs are fabricated by solvothermal route using *EGCG* as bio-surfactant. Chemicals used for the synthesis of $ZnAl_2O_4$: Ho^{3+} NPs were of analytical grade Zinc nitrate [$Zn(NO_2)_3.6H_2O$], Aluminium nitrate [$Al(NO_3)_3.6H_2O$] and Holmium nitrate [$Ho(NO_3)_3.5H_2O$] purchased from Sigma Aldrich and were used without further purification. The bio-surfactant EGCG was extracted as per the literature [11]. Stoichiometric quantities of Zinc nitrate, Aluminum nitrate and Holmium nitrate are thoroughly dissolved in 20 ml ethanol using magnetic stirring for ~10 min. Consequently, 5 ml of *EGCG* surfactant is mixed with precursor solution. The resultant solution was transmitted to Teflon-lined autoclave (100 ml), sealed and maintained to ~ 180 °C for different reaction times (12 h) and thereafter allowed to cool naturally up to room temperature. A white solid product was followed by filtration, washed several times with distilled water and ethyl alcohol and then dried at 80 °C. The obtained product was calcined at ~700 °C for 3 h and used for further studies.

2.2. Characterization

The Shimadzu made X-ray powder diffractometer (PXRD - 7000) using Cu-Kα (1.5406 Å) radiation with a nickel filter was used structural characterization of the prepared samples. Morphological studies were carried by scanning electron microscope (SEM, Hitachi-7000 model) and transmission electron microscope (TEM, TECNAI F-30). The diffuse reflectance of the samples was performed using Lambda −35, Perkin Elmer in the wavelength range 200–1100 nm. PL studies were performed on a Jobin-Yvon Flurolog-3 Spectrofluorimeter using 450 W, Xenon lamp as an excitation source. The Nucleonix TLD reader was used to record TL glow peaks by irradiating γ - rays in the dose range 0.25–15 kGy.

3. Results and discussion

3.1. Structural analysis

Fig. 1(a) depicts the PXRD profiles of $ZnAl_2O_4$: Ho^{3+} (0.25–5 mol %) NPs. All diffraction profiles (220), (311), (400), (331), (422), (511) and (440) corresponds to cubic structure of $ZnAl_2O_4$ and were well matched with JCPDS card No. 05–0669. No other impurity peaks were observed which indicates that the substitution of Ho^{3+} ions did not influence the crystal structure and phase of the samples. The average crystallite size (D) of the products was estimated by using Scherrer's relation [12];

$$D=\frac{0.9\,\lambda}{\beta\cos\theta} \quad (1)$$

where β; full width at half maxima (FWHM) in radian, λ; wavelength of X-ray used (1.542 Å), θ; Bragg's angle. The 'D' values of the prepared samples were estimated and tabulated in Table 1. The line broadening in diffraction peak is associated with 'D' values or the strains within the sample or both. The W-H plot method was also employed to estimate the 'D' values as well as the strain present in the prepared samples were estimated by using following relation [13]:

$$\frac{\beta cos\theta}{\lambda}=\frac{k}{D}+\frac{\varepsilon sin\theta}{\lambda} \quad (2)$$

where ε; strain associated with NPs. Assume Eq. (2) represents a straight line between 4sinθ (X-axis) and βcosθ (Y-axis). The slope of the line gives the strain (ε) and intercept (kλ/D) of this line on Y-axis gives 'D' values (Fig. 1(b)). The calculated values of 'D' and strain were tabulated in Table 1.

Table 1
Estimated crystallite size, micro strain and energy gap of $ZnAl_2O_4$:Ho^{3+} (0.25–5 mol %) NPs.

Ho^{3+} Conc. (mol %)	Crystallite size (nm)		Micro strain $\times 10^{-3}$	Energy gap (eV)
	Scherrer's	W-H Plot		
0.25	16	18	3.74	3.55
0.5	18	21	1.79	3.65
1	19	23	2.13	3.49
3	20	25	3.70	3.61
5	17	20	4.17	3.71

3.2. Diffuse reflectance spectral studies

Fig. 2(a) shows the DR spectra of $ZnAl_2O_4$:Ho^{3+} (0.25–5 mol %) NPs. Several prominent peaks were recorded at ~420, 450, 480, 540 and 650 nm, which may be due to $^5I_8 \rightarrow {}^5G_5$, $^5I_8 \rightarrow {}^5G_6$, $^5I_8 \rightarrow {}^5F_3$, $^5I_8 \rightarrow {}^5S_2$ and $^5I_8 \rightarrow {}^5F_5$ transitions of the Ho^{3+} ions, respectively [14]. The

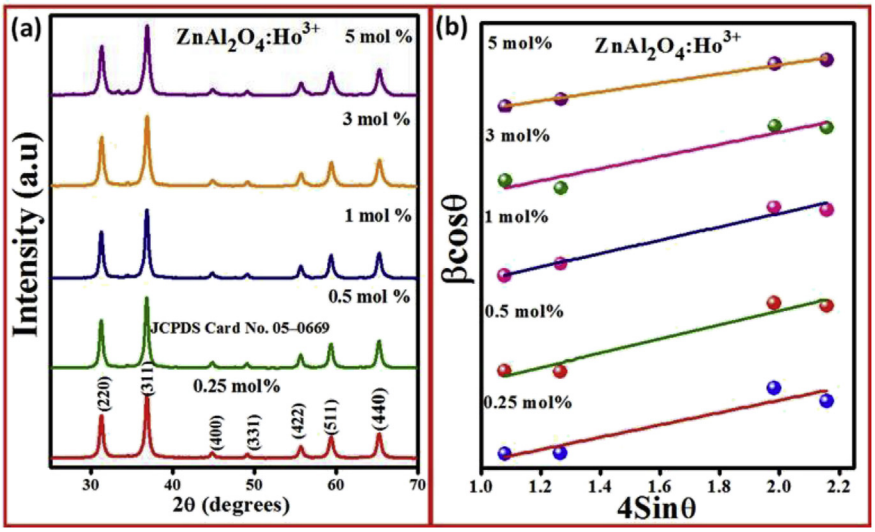

Fig. 1. (A) PXRD patterns and (b) W-H plots of $ZnAl_2O_4$:Ho^{3+} (0.25–5 mol %) NPs.